Astron. Astrophys. 321, 605–617 (1997)

ASTRONOMY
AND
ASTROPHYSICS

Carbon stars with detached dust shells: the circumstellar envelope of UU Aurigae

S. Bagnulo[1], **C.J. Skinner**[2], **J.G. Doyle**[1], **and M. Camphens**[3]

[1] Armagh Observatory, College Hill, Armagh BT61 9DG, Northern Ireland (sba@star.arm.ac.uk & jgd@star.arm.ac.uk)
[2] Space Telescope Science Institute, 3700 San Martin Drive, Baltimore MD 21218, USA (skinner@stsci.edu)
[3] Sterrekundig Instituut, Postbus 8000, 3508 TA Utrecht, The Netherlands (M.Camphens@fys.ruu.nl)

Received 1 March 1996 / Accepted 24 October 1996

Abstract. We have modelled the spectral energy distribution of the carbon-rich star UU Aurigae, which shows an excess flux in the far infrared and sub-millimeter regions, in terms of a detached shell generated by an episode of higher (than the current) mass loss rate. Two different compositions for the detached shell were used: oxygen-rich and carbon-rich dust grains. By assuming that at longer wavelengths the extinction coefficients of the oxygen-rich grains follow a λ^{-2} law, and those of the amorphous carbon follow a $\lambda^{-1.3}$ law, we show that the model including a detached carbon-rich shell produces a more satisfactory fit to the observational data compared to the model with a detached oxygen-rich shell. Moreover, we derived a relatively small value for the distance of the detached shell from the central star, which implies that the episode of high mass loss rate ended only few hundred years ago.

The results of our analysis are consistent with the scenario for the stellar evolution on the asymptotic giant branch which predicts a short time-scale modulation of the mass loss rate induced by repeated Helium shell-flashes.

Key words: stars: carbon – circumstellar matter – stars: individual: UU Aur

1. Introduction

Asymptotic giant branch (AGB) stars are evolved low or intermediate mass objects which show copious mass loss. Dust grains form in the cool expanding circumstellar environment, absorb the optical radiation of the parent star, and re-emit in the infrared (IR). The chemical nature of the dust grains in a stellar wind depends on the composition of the stellar photosphere. Grains of carbon compounds such as amorphous carbon (AC) and silicon carbide (SiC) surround C-rich stars, while silicate constitutes the main component of the dust around O-rich stars (Savage & Mathis 1979).

Send offprint requests to: S. Bagnulo [sba@star.arm.ac.uk]

In the last decade it has been well established that many carbon stars – especially those optically visible – show excess flux in the far-IR (e.g., Thronson et al. 1987, Chan & Kwok 1988, Willems & de Jong 1988). Based on the present knowledge of the optical properties of the dust grains in the far-IR, and assuming that the mass loss rate is constant with time, in many cases one is not able to explain the flux at 60 and 100 μm measured by the Infrared Astronomical Satellite (IRAS).

Recently, Van der Veen et al. (1995) found that 4 AGB stars (among a sample of 11 detected in the sub-mm range), have fluxes greater by a factor 3–5 than what can be explained with a constant mass loss model. Three out of the 4 stars with far-IR flux excess have an optically thin shell at shorter wavelengths.

Several reasons can be invoked to explain the observed sub-mm excess: contribution of molecular lines, free-free emission, or mass loss variability. Here we follow the approach of reproducing the large excess flux observed at the longer wavelengths (from 60 μm to the millimeter), by attributing it to the presence of a large dust shell emitting at these wavelengths, produced by past episodes of mass loss.

Indeed, the idea that sudden mass loss changes may occur in C-rich stars is not new. In particular, two kinds of scenarios were suggested in recent years, both of them based on the assumption that the excess flux is emitted by a detached remnant shell ejected in a previous episode of high mass loss rate. However, these scenarios disagree on the typical size and chemical composition of the detached shell, and on the physical processes which cause its formation.

Willems & de Jong (1988) hypothesized that most of the detached shells are O-rich. During the AGB evolution, an M Mira variable star produces a silicate shell. Triggered by a thermal pulse, carbon becomes more abundant than oxygen in the stellar photosphere, and the mass loss drops suddenly. The silicate shell expands far away from the star, while an inner C-rich shell is generated via a low mass loss rate. Eventually the mass loss rate increases and – on a time-scale of 10^4 years – the circumstellar C-rich environment obscures the parent star. Optical carbon stars – including those few which show a silicate feature

in their mid-IR spectrum (Willems & de Jong 1986) – would be objects at an intermediate evolutionary phase, i.e., after the O-rich phase and before they form a thick C-rich dust shell. Based on a statistical approach, there have been several studies supporting this theory. For example, Egan & Leung (1991) considered a sample of 125 C-rich stars taken from the IRAS Low Resolution Spectrometer (LRS) catalogue, performed radiative transfer calculations, and compared their results to the IRAS colour-colour diagrams. Their picture of the circumstellar envelopes around C-rich stars is a two-shell structure, where the outer shell has an inner radius of 0.1 pc and an outer radius of 1 pc. Based on considerations about the time-scale required by their models, their conclusions were in favour of the Willems & de Jong (1988) theory.

An alternative scenario is supported by Zuckerman (1993), along with other researchers (e.g., van der Veen & Habing 1988, Olofsson et al. 1990) who suggest that most detached envelopes are C-rich, (some with multiple structure), and are due to thermal pulses which suppress for some time the dynamical pulsation and also the mass loss. Apart from the different origin and chemical composition of the outer shell, a notable disagreement with the previous scenario concerns the size of the dust shells. Modelling of CO emission by Olofsson et al. (1990, 1992), and spectral and spatial distribution of the IRAS broadband photometry by Hawkins (1990, quoted by Zuckerman 1993), yield for the outer radius of the C-rich circumstellar envelopes values about ten times smaller than those estimated by Egan & Leung (1991).

C-rich stars with a hollow circumstellar shell (or even multiple shells) are also predicted by Vassiliadis & Wood (1993), who suggest that in low mass AGB stars ($M \lesssim 2.5 M_{\odot}$), the mass loss rate is negligible *except* during the last few shell flash cycles. Some AGB stars would undergo a period of high mass loss rate, preceded and followed by longer periods of low mass loss rate.

We decided to approach the problem concerning the nature of the outer shell (or shells) by focusing our attention on one star, and showing how different models (consistent with the scenarios quoted above) compare to the observed spectral energy distribution (SED). The target selected was UU Aurigae, an optically identified carbon star with a large far-IR excess. We obtained a mid-IR low resolution spectrum at the United Kingdom Infrared Telescope, and a photometric measurement in the sub-mm at the James Clerk Maxwell Telescope. Our data, together with optical and near-IR photometry taken from the literature and the IRAS broadband photometry, provide a coverage of the observable SED spanning from 0.44 μm to 0.8 mm.

We consider a number of different hypotheses concerning the nature of the dust shell, that is, we assume different dust components (SiC, AC and silicate) and different kinds of spatial distributions for the dust grains, then we compare and discuss the resulting best-fits.

2. Method

2.1. Radiative transfer code

The analysis carried out in this paper is based on the modelling technique described in Bagnulo et al. (1995).

A FORTRAN code originally developed by Haisch (1979) – with several upgrades – solves the radiative transfer equation in a spherically symmetric medium, taking into account the absorption and scattering properties for a multiple dust grain composition, and multiple size distribution. The zero, first and second order moments of the transfer equation are numerically solved under a generalized two-stream Eddington approximation due to Unno & Kondo (1976).

The model SED is then compared to the observed broadband photometry (from the optical to mm wavelengths), and to low resolution mid-IR spectrum.

2.2. Inputs

The inputs to this code are as follows.
i) The radius R_*, the effective temperature T_*, and the distance d_* of the central star, the radiation field of which is approximated by that of a blackbody. Obviously, these three parameters are not independent, since combined they have to account for the apparent stellar luminosity.
ii) The inner and outer radii of each dust component.
iii) The absorption and scattering cross-sections for each dust component.
iv) The size distribution of the dust grains.
v) The spatial density distribution of the dust grains.

2.3. Outputs

The most significant output is the emerging flux, which is compared to the broadband photometric and spectro-photometric measurements. Grain temperature distributions and surface brightness profiles are also provided by the code.

2.4. Comparing theoretical models and observational data

When we attempt to reproduce both the spectral features observed in the mid-IR and the general shape of the whole SED, the definition of the "best-fit" to the observational data is not obvious. This is because we usually cannot find a unique model reproducing all the observational data ranging from the optical to the sub-mm. Often, a model which produces the best-fit to the spectro-photometric data, cannot account for the overall SED, or, vice versa, a model which reproduces the general shape of the spectral distribution does not fit the low-resolution spectral features. Therefore we are forced to seek a model which represents a "reasonable compromise" between the two. The best-fit parameters however, can differ depending on what we consider as "reasonable compromise". The strategy adopted is described below.

We assign *a priori* an error of 25 % to the ground-based photometric data. Of course, at shorter wavelengths, magnitudes are

determined with much more precision; the large value for the error that we estimate is due to the uncertainty of deriving the flux at the effective wavelengths from the broadband photometric measurements (see, e.g., Bergeat et al. 1976).

Broadband photometry at 12, 25, 60 and 100 μm taken by IRAS is considered with the original error declared in the IRAS Point Source Catalog (1986) (in the present case, 4 %, 4 %, 10 % and 11 %, respectively). Such measurements were colour corrected by convolving the model spectra with the filter responses tabulated in the *Explanatory Supplement* (Joint IRAS Science Working Group 1986).

We calculate a number of theoretical models, considering different numerical values as input parameters. For each model we calculate three contributions to the total χ^2 defined by the three spectral regions, namely:
– the contribution $\chi^2_{\rm NIR}$ due to the broadband photometric measurements with $\lambda \leq 10\,\mu$m;
– the contribution $\chi^2_{\rm SPECT}$ due to the spectro-photometric measurements;
– the contribution $\chi^2_{\rm FIR}$ due to the broadband photometric measurements with $\lambda > 10\,\mu$m.

In fact, we do not take into account the broadband photometric measurements at the wavelengths covered by the mid-IR spectrum, in the present case, those from 7 to 24 μm.

In the millimeter regions beam-size effects may become important since the beam used to observe the source could be smaller than the angular extent of the object. Therefore the measurement in the sub-mm was compared to the model spectra convolved with a Gaussian of FWHM = 18.5 arcsec (see Sect. 4.3).

The absolute calibration of the spectro-photometric measurements is made consistent with the particular SED model by multiplying the measured flux by a scaling-factor f which minimises the value of $\chi^2_{\rm SPECT}$, but we reject the models for which the condition $0.9 < f < 1.1$ is not satisfied. This approach is consistent with taking for the mid-IR spectrum an absolute calibration uncertainty of 10 %. We mention here that for all the models presented in this paper, this factor was about 1.1. After this correction, the absolute mid-IR spectrum was always fully consistent with the colour-corrected 12 μm IRAS broadband photometry.

We deem as "a reasonable model" one which produces a fit with all the above defined χ^2 – divided by the number of relevant measurements, about 1.

Let us consider a shell composed of dust grains having radius a, with a number density $\propto r^{-2}$, r being the distance from the central star. The absorption and scattering coefficients, $k_\lambda(a,r)$ and $\sigma_\lambda(a,r)$, respectively, are function of the dust mass loss rate, $\dot{M}_{\rm d}$, of the density of the grain material, $\rho_{\rm d}$, of the velocity of the out-flowing dust, $v_{\rm d}$, and of the absorption and scattering efficiency factors, $Q_{\rm abs}(a,\lambda)$ and $Q_{\rm sca}(a,\lambda)$, respectively. They can be written as

$$k_\lambda(a,r) = \mathscr{A}\frac{Q_{\rm abs}(a,\lambda)}{a}\frac{1}{r^2}$$
$$\sigma_\lambda(a,r) = \mathscr{A}\frac{Q_{\rm sca}(a,\lambda)}{a}\frac{1}{r^2}\ ,$$

where

$$\mathscr{A} = \frac{3}{16\pi}\frac{1}{\rho_{\rm d} v_{\rm d}}\dot{M}_{\rm d}\ . \quad (1)$$

Once the stellar parameters and the optical constants of the dust grains have been fixed, it is possible to derive $\mathscr{A}$ by comparing the model SED with the observations. Then, from Eq. (1), one can derive the dust mass loss rate if $\rho_{\rm d}$ and $v_{\rm d}$ are known, and estimate the dust-to-gas ratio if the gas mass loss rate, $\dot{M}_{\rm g}$, is also known.

It should be noted that, in most cases, stellar parameters are not well determined. In the present case, the angular diameter of UU Aur is known via direct measurements (see Sect. 5.2), thus, from the broadband photometry, we can obtain the stellar effective temperature. Instead, the distance is only estimated by *a priori* setting a value for the absolute luminosity of the star.

Let us consider a star of radius R'_* to a distance d'_*, surrounded by a dust shell with an inner radius of $R_{\rm inn} = R'_{\rm inn}$, outer radius $R_{\rm out} = R'_{\rm out}$, and characterised by a value $\mathscr{A} = \mathscr{A}'$. Let us consider a second star with the same effective temperature as the previous one, having radius R''_*, to a distance d''_*, and surrounded by a shell composed of the same kind of dust grains, and characterised by $R_{\rm inn} = R''_{\rm inn}$, $R_{\rm out} = R''_{\rm out}$, and $\mathscr{A} = \mathscr{A}''$. The relevant SEDs predicted for these two systems are identical if the parameters quoted above differ by the same scaling-factor α, that is, if $R''_* = \alpha R'_*$, $d''_* = \alpha d'_*$, $R''_{\rm inn} = \alpha R'_{\rm inn}$, $R''_{\rm out} = \alpha R'_{\rm out}$, $\mathscr{A}'' = \alpha.\mathscr{A}'$. Therefore, once the effective temperature and the angular diameter of a star are fixed, the quantity actually derived via spectral analysis is the ratio $\mathscr{A}/d_*$ (or $\mathscr{A}/R_*$).

3. Optical constants of the dust grains

Amorphous carbon, SiC and silicate were considered as possible components of the dust shell. Absorption and scattering cross-sections were derived via Mie-Theory adopting suitable runs of optical constants which are presented in the following.

We assumed the density of the dust grains to be 1.8, 3.2 and 3.0 g cm^{-3} for AC, SiC and silicate, respectively.

3.1. Amorphous carbon

Optical properties of AC have been extensively investigated in the laboratory by several authors (e.g. Koike et al. 1980, 1994; Bussoletti et al. 1987; Blanco et al. 1991; Colangeli et al. 1995).

Rouleau & Martin (1991) derived four sets of optical constants from the extinction data of the AC samples produced in the laboratory by Bussoletti et al. (1987). In this work we consider those labeled with "AC1" in their Table 1. At wavelengths shorter than 100 μm, the absorption coefficients follow a power law in $\lambda^{-\beta}$ with spectral index $\beta \simeq 1$, which rises up to $\simeq 1.8$ at the two last data points tabulated by the authors (λ = 283 and 300 μm). In order to calculate the absorption cross-sections at wavelengths longer than those considered by the authors, we decided though to base an extrapolation on all data points tabulated from λ = 250 μm to λ = 300 μm. The spectral index so derived is $\beta \simeq 1.3$.

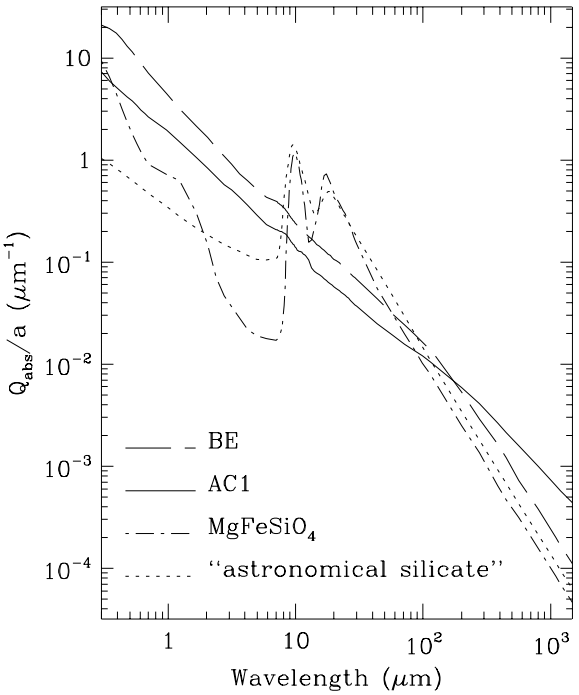

Fig. 1. Absorption coefficients per unit of grain radii vs. wavelength, for various dust species. The grain radius is set to 5 10^{-3} μm. Long-dashed line: "BE" sample of AC, optical constants calculated by Preibisch et al. (1993). Solid line: "AC1" sample, optical constants calculated by Rouleau & Martin (1991). Dot-dashed line: $MgFeSiO_4$, optical constants given by Dorschner et al. (1995). Dotted line: "astronomical silicate", optical constants given by Draine (1985). At longer wavelengths, the absorption coefficients are derived basing on an extrapolation on the last data points tabulated by the authors (see text)

Preibisch et al. (1993) published a set of optical constants derived from the laboratory measurements by Bussoletti et al. (1987) and by Blanco et al. (1991), which extend up to 800 μm, and, at longer wavelengths, the spectral index is $\beta \simeq 1.9$.

In Fig. 1 we compare the absorption coefficients derived from the optical constants given by Rouleau & Martin (sample AC1, solid line) with those derived from the optical constants calculated by Preibisch et al. (1993) (sample "BE", long-dashed line). At 1 μm, the absorption coefficients of the sample AC1 are smaller by a factor 2 than those of the BE sample.

It should be noted that the extinction curve derived from the laboratory measurements carried out in other works exhibit a smaller spectral index at longer wavelengths. Tanabé et al. (1983) report for hydrogenated AC grains a spectral index $\beta = 0.6$ in the far-IR, a value consistent with that derived by Colangeli et al. (1995), who give $\beta \simeq 0.5$ in the range $\lambda = 30 - 180\,\mu$m, and $\beta \simeq 1.1$ in the range $340 - 1100\,\mu$m. Extinction cross-sections are actually dependent on the laboratory conditions of production of the sample of dust grains. Modelling of observed SEDs of a large number of objects is required in order to establish which particular form of AC (or hydrogenated AC) is more likely produced in the circumstellar environments of C-rich stars.

In this work we adopted the absorption and scattering coefficients derived from the optical constants given by Rouleau & Martin (1991).

3.2. Silicon carbide

Silicon carbide exists in two crystallographic forms, referred to as α-SiC (hexagonal/rhomboedric), and β-SiC (cubic). Baron et al. (1987) and Papoular (1988) favoured α-SiC to explain the shape of the feature seen in the low-resolution spectra of C-rich stars. Groenewegen (1995) also found that mid-IR spectra of 19 out of 21 C-rich stars he modelled were fitted with α-SiC.

Here we adopted the optical constants for α-SiC given by Pégourié (1988), which were synthesized on the basis of laboratory measurements carried out by Phillip & Taft (1969) and by Borghesi et al. (1985, 1986). At wavelengths longer than $\simeq 170\,\mu$m, the slope of the extinction curve is constant, with a spectral index $\beta \simeq 2$. The data points beyond 244 μm were extrapolated by adopting this value for the spectral index.

3.3. Silicate

A large number of laboratory measurements and theoretical calculations have been made on O-rich grains. A comprehensive collection of optical constants for silicate grains has been presented by Draine & Lee (1984) and Draine (1985) (see also Laor & Draine 1993). This set of optical constants was synthesized by requiring that the grain optical properties were consistent with a number of constraints obtained from both astronomical observations and laboratory measurements. The absorption coefficients follow a $\lambda^{-\beta}$ law, with $\beta = 2$, for $\lambda \gtrsim 20\,\mu$m. Such a behaviour at longer wavelengths is consistent with that of the absorption cross-sections of several kinds of silicate obtained from laboratory measurements. Magnesium-iron silicates studied by Day (1981) follow a power law with $\beta = 1.8$ from $\lambda = 100\,\mu$m to $\lambda = 300\,\mu$m. Magnesium-iron silicates studied by Dorschner et al. (1995) have $\beta = 2$ for $\lambda \gtrsim 70\,\mu$m. Fig. 1 shows the absorption coefficients per unit of grain radii derived from the optical constants for astronomical silicate given by Draine (1985) (dotted line) and for the olivine $MgFeSiO_4$ presented by Dorschner et al. (1995) (dot-dashed line).

In the present work we adopted the set of optical constant given by Draine (1985).

4. Size of the dust grains

Since the dust ejected by evolved late-type stars is a major component of the interstellar matter, the size distribution of circumstellar dust grains must be related to that of the interstellar dust grains. The standard model of Mathis et al. (1977) for the interstellar medium predicts that dust grains have a radius a ranging approximately from 5 10^{-3} to 0.25 μm, following a distribution $\propto a^{-3.5}$. The existence of a few larger grains is not excluded by other authors (see e.g. Kim et al. 1994), but it is widely accepted that most of the interstellar grains have a relatively small

size (e.g., the mean radius predicted by the size distribution proposed by Mathis et al. 1977 is $\simeq 8\,10^{-3}\,\mu$m). By contrast, it is unclear whether such small grains are formed in circumstellar environments, or if they are produced in interstellar space by shock fragmentation. Seab & Snow (1989) modelled the observed ultraviolet extinction curve for the circumstellar dust of the red supergiant α Scorpii concluding that no silicate grains smaller than $8\,10^{-2}\,\mu$m are present.

Sorrel et al. (1990) suggested that AC grains with radius larger than $0.05\,\mu$m will be destroyed by hydrogenation and chemical sputtering in dense clouds. Groenewegen (1997) fitted the visibility data of IRC +10 216 by adopting AC grains with a radius of $0.16\,\mu$m. Therefore, we assumed that the mean radius of AC grains was definitely not larger than few $0.1\,\mu$m. However we were not able, with the available photometry at shorter wavelengths, to determine the best size distribution for the dust grains. In fact, in the present analysis we considered all the grains having the same radius, which was set to $5\,10^{-3}\,\mu$m. For grains so small, even at the shortest observed wavelengths, the scattering is negligible, and the absorption coefficients (in units of grain radii) are independent of the grain radius. In Sect. 7 we will also discuss the cases of dust shells composed of grains having radii of $0.25\,\mu$m, and having a size distribution like the one suggested by Mathis et al. (1977). Since the present work is focussed on the analysis of the large far-IR and sub-mm excess observed in the SED of UU Aur, the main results will not be affected by the choice of grain size, provided that most of the grains composing the circumstellar envelope have a radius not much larger than $1\,\mu$m. This is because the wavelengths at which the (cool) dust grains of the outer shell emit are much larger than the grain radius. With this condition satisfied, transport coefficients and the calculated emerging flux are independent of the grain size.

5. Parameters of UU Aurigae

5.1. Spectral type

UU Aurigae is a carbon star of spectral type C 6,4, according to the classification by Yamashita (1972).

5.2. Effective temperature

Quirrenbach et al. (1994) measured the angular diameter of this star, giving the value (corrected for limb-darkening) of $\theta = 12.07 \pm 0.22$ mas. Then they inferred – based on the bolometric flux – an effective temperature $T_* = 2767 \pm 25$ K, which is in good agreement with the value of 2825 K obtained by Tsuji (1981) via the infrared flux method.

5.3. Distance

Two parallax estimates are given by the Simbad database, 0.002 ± 0.001 and 0.003 ± 0.001, from which we obtain that the distance of UU Aur is ranging from 250 to 1000 pc.

Frogel et al. (1980) found that N type C-rich stars in the Magellanic Cloud clusters have an absolute J magnitude of $\simeq -8.1$. By adopting the same absolute magnitude for UU Aur, Olofsson et al. (1987) derived a value for the distance of 290 pc, which is in agreement with both the value of 270 pc given by Groenewegen et al. (1992) (derived by assuming for UU Aur an absolute luminosity of $7050\,L_\odot$), and the value of 320 pc adopted by Knapp (1986).

Loup et al. (1993) quote the value of 1200 pc which is not consistent with the adopted photometric data (see Sect. 6). This would result in a star with a luminosity of $140,000\,L_\odot$, which is almost an order of magnitude above the theoretical AGB limit.

5.4. Mass loss rate

To estimate the dust-to-gas ratio of the different dust components requires knowledge of the gas mass loss rate.

Based on a CO $J = 1 - 0$ line detection, Knapp (1986) derived a gas mass loss rate of $2.9\,10^{-7}\,M_\odot\,\mathrm{yr}^{-1}$, consistent with the value of $2.8\,10^{-7}\,M_\odot\,\mathrm{yr}^{-1}$, obtained by Olofsson et al. (1987). More recently though, Olofsson et al. (1993) derived the value of $1.3\,10^{-7}\,M_\odot\,\mathrm{yr}^{-1}$. Olofsson et al. (1993) show also CO line profiles, which do not appear double peaked (see discussion in Sect. 9).

Groenewegen et al. (1992) found that the general formula used to derive the mass loss rate from CO line detection (see, e.g., Eq. (10) of Groenewegen et al. 1992) yields systematically higher values for non resolved envelopes (as that of UU Aur), and, after analysing further the previous measurements, they propose the value of $8.0\,10^{-8}\,M_\odot\,\mathrm{yr}^{-1}$. On the other hand, Olofsson et al. (1993) suggest that the same formula *underestimates* the gas mass loss rate, especially for small values of $\dot{M}_\mathrm{g}$, and more detailed models of circumstellar CO by Kastner (1992) provide mass loss rate for low-$\dot{M}_\mathrm{g}$ objects higher by a factor 2 than those obtained by using the general formula quoted above. We note that the discrepancies between the values of $\dot{M}_\mathrm{g}$ quoted above can be partially reduced by scaling them like d_*^2. However, the value for the ratio $\dot{M}_\mathrm{g}/d_*^2$ as derived by Groenewegen et al. (1992) (namely, $1.1\,10^{-12}\,M_\odot\,\mathrm{yr}^{-1}\,\mathrm{pc}^{-2}$) is 2/3 of the value derived by Olofsson et al. (1993) and 2/5 of the value derived by Knapp (1986).

5.5. Out-flowing dust velocity

In order to derive the mass loss rate for the dust, we need to know the value of the velocity v_d of the out-flowing dust.

The velocity of the out-flowing gas, v_g, as given by Knapp (1986), is $13.4\,\mathrm{km\,s}^{-1}$, while both Groenewegen et al. (1992) and Olofsson et al. (1993) derived a value around $11\,\mathrm{km\,s}^{-1}$.

In general, we cannot assume that the dust velocity is equal to the gas velocity, since it is known that dust grains move with a drift velocity relative to the gas. Such a drift velocity is definitely negligible with respect to the gas velocity only in optically thick shells with mass loss rates of $\sim 10^{-5}\,M_\odot\,\mathrm{yr}^{-1}$ or higher. On the contrary, UU Aur is surrounded by an optically thin shell, with a rather small gas mass loss rate.

Detailed calculations of two-fluid models for stationary dust-driven winds carried out by Krüger et al. (1994) show

Table 1. Parameters for UU Aur as given by different authors. The stellar radius is consistent with the distance, the adopted value for the effective temperature of 2767 K, and the photometry. The meaning of the scaling-factors g_1 and g_2 are explained in the text (Sect. 5.6)

distance (pc)	$\dot{M}_{\rm g}$ ($M_\odot$ yr^{-1})	$v_{\rm g}$ km s^{-1}	R_* ($R_\odot$)	g_1	g_2	Ref.
290	$1.3\,10^{-7}$	10.9	370	1.00	1.00	1
270	$8.0\,10^{-8}$	11.4	340	0.95	1.55	2
320	$2.9\,10^{-7}$	13.4	410	1.35	0.60	3

Key to references. 1: Olofsson et al. (1993); 2: Groenewegen et al. (1992); 3: Knapp (1986)

that, for a star of $10^4\,L_\odot$ and gas mass loss rate of $\sim 4.4\,10^{-6}\,M_\odot$ yr^{-1}, the drift velocity is less 1 km s^{-1} for grains of radius $a = 0.012\,\mu$m, and less than 10 km s^{-1} for grains of radius 0.25 μm. Assuming that the grain drift velocity depends on $(L/\dot{M}_{\rm g})^{1/2}$, for grains with radius $5\,10^{-3}\,\mu$m as adopted in this work, the grain drift velocity is probably negligible, compared to the gas velocity. If the grain drift velocity is non-negligible, then the dust-to-gas ratios determined later in this work will be underestimated.

5.6. Adopted parameters for UU Aurigae

We adopted for UU Aur the effective temperature and the stellar angular diameter as given by Quirrenbach et al. (1994), which are fully consistent with the set of photometric data that we have considered (see Sect. 6).

For the sake of clarity, in the following we will describe our results by quoting the mass loss rates and dust-to-gas ratios as derived by setting $v_{\rm d} = v_{\rm g}$, and by adopting the set of parameters $v_{\rm g}$, $\dot{M}_{\rm g}$, d_* and R_* given by Olofsson et al. (1993) (the stellar radius $R = 370\,R_\odot$ is derived from the observed SED).

The dust mass loss rates and dust-to-gas ratios that would be obtained by adopting different parameters for $v_{\rm d}$, $\dot{M}_{\rm g}$, d_* and R_* can be obtained simply by multiplying the values that we are going to quote by suitable scaling-factors. Namely, from the mass loss rate $\dot{M}_{\rm d}$ as derived by adopting the parameters given by Olofsson et al. (1993), one can derive the mass loss rate for the parameters given by Groenewegen et al. (1992) or by Knapp (1986), by multiplying $\dot{M}_{\rm d}$ by $g_1 = 0.96$, or $g_1 = 1.36$, respectively. Similarly, the dust-to-gas ratios as calculated by adopting the parameters given by the other authors can be obtained by multiplying the dust-to-gas ratio derived from the parameters of Olofsson et al. (1993) by $g_2 = 1.55$, (for the data of Groenewegen et al. 1992) or $g_2 = 0.60$ (for the data of Knapp 1986) (see Table 1).

6. Observations of UU Aurigae

6.1. Selection of the ground-based broadband photometric measurements

Among the ground-based photometric measurements published in the literature, we used those gathered in Table 4 of Bergeat et al. (1976) spanning from 0.44 μm to 20.0 μm. Measurements given by Fernie et al. (1983) and by Noguchi et al. (1981) are not in agreement with Bergeat et al.'s set of measurements, possibly due to the variability of the star.

6.2. Mid-IR spectra

A low-resolution mid-IR spectrum ($R = \lambda/\Delta\lambda = 60$) of UU Aur was obtained at the 3.8 m United Kingdom Infrared Telescope (UKIRT) on 30 October 1993 using the common-user mid-IR spectrometer CGS3. An $8 - 13\,\mu$m spectrum was taken in the usual manner, chopping the secondary 15" E–W at 5 Hz and nodding E–W at 10 second intervals in order to remove thermal background emission. Atmospheric features were removed using spectra of the standard star α Tau. It was not possible to obtain a $16 - 24\,\mu$m spectrum due to inadequate sky conditions. With a similar technique, we observed UU Aur once again on 21 and 22 August 1995. This time we managed to take both a $8 - 13\,\mu$m and a $16 - 24\,\mu$m spectrum of good quality. The spectra of UU Aur were obtained as part of a survey of mid-IR spectra of C-rich stars, the results of which will be presented in a forthcoming paper.

Fig. 2 shows both our CGS3 spectra compared to that of the IRAS LRS catalogue, and the IRAS broadband photometry at 12 and 25 μm colour corrected according to the model shown in Fig. 2. The absolute calibration of the more recent spectrum taken at the UKIRT (solid line) is fully consistent with that of the spectrum taken in 1993, while the absolute flux measured by the IRAS LRS (Joint IRAS Science Working Group 1986) is about 15 % higher. Since the IRAS flag for the mid-IR variability of UU Aur is 0/10, these small discrepancies can probably be ascribed to uncertainty in the absolute calibration.

In our analysis we used the more recent CGS3 spectrum.

6.3. A sub-millimeter measurement

A measurement at $\lambda = 0.8$ mm was obtained on 9 December 1994 using the common-user instrument UKT14 at the Nasmyth focus of the James Clerk Maxwell Telescope (JCMT) on Mauna Kea, Hawaii. UKT14 is a ^{3}He-cooled, single-channel bolometer with filters that cover all major sub-millimeter windows. Using an aperture of 65 mm gives a beam width of ~ 18.5 arcsec in all filters. Sky subtraction was achieved via a chopping secondary, using a chop of 60 arcsec in azimuth with a frequency of 7.8 Hz. For flux calibration we used Saturn as a primary calibrator and CRL 618 as the secondary, The flux for Saturn was derived using the JCMT utility program FLUXES. UU Aur was observed at $\lambda = 0.8$ mm, and a flux of 78 ± 20 mJy was measured.

7. The flux excess of UU Aurigae

A common modelling technique pictures carbon stars as blackbodies surrounded by dust shells with an inner radius of a few stellar radii (e.g. Lorenz-Martins & Lefèvre 1993, 1994), composed of SiC and/or AC grains (or graphite instead of AC), with a r^{-2} number density, implying a constant mass loss rate.

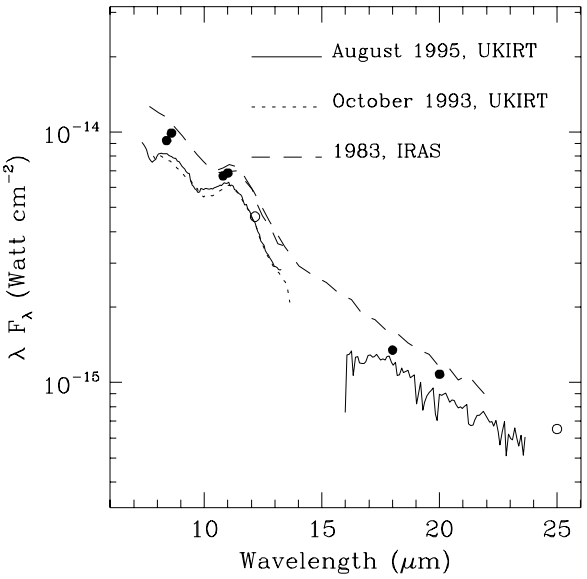

Fig. 2. Mid-IR low resolution spectra of UU Aur. The solid line shows the CGS3 spectrum taken at the UKIRT on 21 and 22 August 1995, the dotted line that taken on 30 October 1993, the long dashed line is the spectrum taken by the IRAS LRS. The empty circles represent the IRAS broadband photometry at 12 and 25 μm (colour corrected according the model of Fig. 2). Filled circles represent the ground-based broadband photometry (see Sect.6.1)

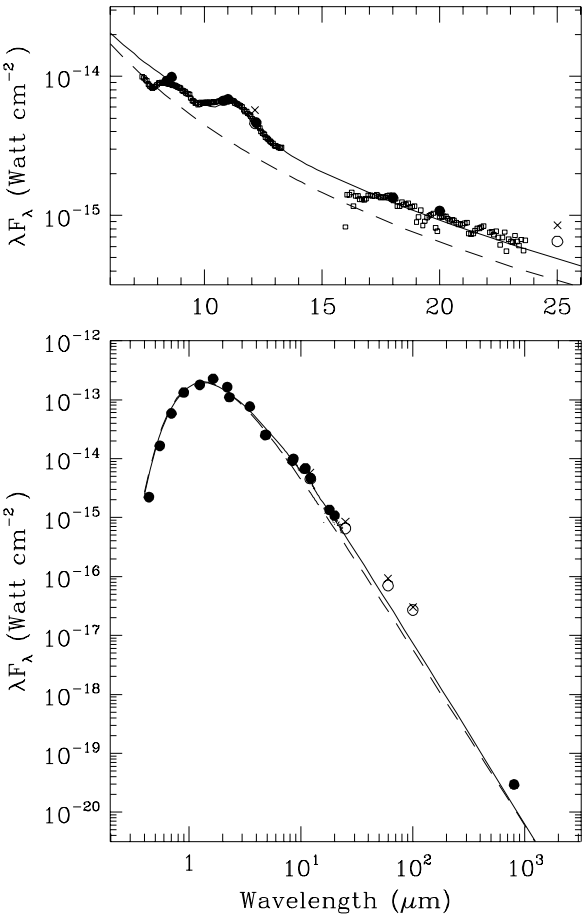

Fig. 3. A model for UU Aur, obtained assuming a shell composed of SiC and AC, produced with a constant mass loss rate. Inner radius for SiC shell is 3 R_*, inner radius for AC shell is 9 R_*, the other parameters are given in the text; note that the SED at longer wavelengths is not accounted for. Filled circles: ground-based photometric measurements (see Sects. 6.1 and 6.3). Empty circles: IRAS broadband photometric measurements at 12, 25, 60, 100 μm, colour-corrected. Crosses: the original IRAS photometry not colour-corrected. Empty squares: UKIRT CGS3 low-resolution spectrum (see Sect. 6.2). The dashed line is the SED of a blackbody of T = 2767 K, which approximates the radiation field of the central star

The hypothesis that C-rich stars are surrounded by dust shells composed of only SiC, as suggested by Le Bertre (1988a, 1988b), probably represents the simplest one in order to explain both the general shape of the SED and the mid-IR spectrum. Chan & Kwok (1990) modelled a large sample of C-rich stars assuming SiC as the sole source of opacity in the circumstellar envelopes. In the case of UU Aur, we were unable to reproduce satisfactorily both the near-IR broadband photometry and the mid-IR spectrum by assuming a dust shell composed exclusively of SiC. On the other hand, we found that the feature around 11 μm could not be reproduced without including SiC. Therefore we tackled the problem of reproducing the SED of UU Aur by adopting a two-component model including both AC and SiC.

Fig. 3 shows one of the best-fits to the near and mid-IR that we obtained. The relevant parameters are as follows. For the SiC shell, inner radius 3 R_* and dust mass loss rate of 6.4 10^{-11} $M_\odot$ yr^{-1}; for the AC shell, inner radius 9 R_* and dust mass loss rate 2.0 10^{-10} $M_\odot$ yr^{-1}. The temperature at the inner radius for SiC and AC shells are 1300 K and 900 K, respectively. The outer radius is 10, 000 R_*. The value of the SiC/AC ratio, 1/3, is consistent with the hypothesis that this quantity may be higher for stars with low mass loss rate than for stars with high mass loss rate (Skinner & Whitmore 1988). The value for $\chi^2_{\rm NIR}$ is 1, ruling out the measurement at 0.44 μm, where the calculated flux is higher by a factor 2.5 than the observed one. The fit to the optical and near-IR broadband photometry could be improved by adopting a lower effective temperature for the star, e.g. setting T_* = 2500 K, which is in disagreement with the direct measurements of T_* presented in Sect. 5.2. Note that we were not able to reproduce the feature seen at 7.8 μm. A similar feature, which may be due to molecular bands in the stellar atmosphere, was also observed in the mid-IR of other visible carbon stars, i.e., EL Aur, RT Cap and R Scl.

The search for the best-fit was repeated by assuming that the dust grains have a radius of 0.25 μm, and keeping the same values of the inner and outer radii as for the model shown in Fig. 3. We found that the dust mass loss rate for both components is reduced to 50 % of the values quoted above. By adopting a size distribution $\propto a^{-3.5}$, having lower limit a = 5 10^{-3} μm and upper limit a = 0.25 μm, we obtained a best-fit for values of the dust mass loss rate intermediate between those ob-

tained assuming that all the grains have a radius $a = 5\,10^{-3}\,\mu$m and those obtained under the assumption that all the grains have a radius $a = 0.25\,\mu$m, i.e., for SiC a dust mass loss of $4.8\,10^{-11}\,M_\odot\,\mathrm{yr}^{-1}$, and for AC a dust mass loss rate of $1.6\,10^{-10}\,M_\odot\,\mathrm{yr}^{-1}$. We were not able to distinguish the best-fit among those obtained with different grain sizes. It should be noted that, for grains of radius $0.25\,\mu$m, the absolute velocity of the out-flowing dust may be almost twice the gas velocity, thus the actual values of the dust mass loss rate for large grains are probably close to those derived for smaller grains.

It was not possible to determine a precise value for the inner radius of the dust shell. Setting the inner radius of the SiC shell to $1.2\,R_*$, and the inner radius of the AC shell to $6\,R_*$, we obtained a reasonable fit with a dust mass loss rate of $6.0\,10^{-11}\,M_\odot\,\mathrm{yr}^{-1}$ for the SiC shell, and of $1.6\,10^{-10}\,M_\odot\,\mathrm{yr}^{-1}$ for the AC shell. The corresponding condensation temperatures are $\simeq$ 2000 K for the SiC grains and $\simeq$ 1000 K for the AC grains. This model produces a slightly better fit to the near-IR photometry, and a slightly worse fit to the mid-IR spectrum than that shown in Fig. 3, but it is not really possible to decide which is the best one. On the other hand, by setting the value of the inner radius for both components to $100\,R_*$, we found that, with a dust mass loss rate of $\simeq 6.5\,10^{-10}\,M_\odot\,\mathrm{yr}^{-1}$ for both AC and SiC, we were still able to reproduce the near-IR photometry and the mid-IR spectrum, although the fit to the feature around $11\,\mu$m is poorer than that shown in Fig. 3. By further increasing the value of the inner radius to values as large as $200\,R_*$, it was still possible to roughly reproduce the shape of feature seen at $11\,\mu$m, but with lack of consistency in the absolute calibration of the mid-IR spectrum and broadband photometry (the factor f required to fit the mid-IR spectrum is about 0.85, and the model predicts about 75 % of the flux at $12\,\mu$m measured by IRAS).

In conclusion, our results are consistent with the hypothesis that the inner radius of the dust shells is a few stellar radii, that is, UU Aur is currently undergoing an episode of (low) mass loss. We were unable to reproduce the observed SED at longer wavelengths. The fit of Fig. 3 predicts at $\lambda = 60\,\mu$m, $100\,\mu$m and 0.8 mm a flux which is respectively about 50 %, 30 % and 40 % of that observed.

It could be argued whether the observed far-IR excess is really due to the dust emission from the circumstellar environment of UU Aur.

Avery et al. (1992) found that 65% of the flux from IRC +10 216 in the range $\lambda \simeq 0.82 - 0.88$ mm is to be ascribed to molecular emission lines.

Confusion flags for cirrus contamination declared in the IRAS Point Source Catalog are CIRR1 = 6 and CIRR2 = 3. The value of CIRR1 might indicate contamination by cirrus with structure on the point source size scale, but the value of CIRR2 estimates the contribution of the cirrus flux less than $\sim$ 6 % of the flux due to the source at $100\,\mu$m. Furthermore, the small value of the ratio CIRR3/F_{60} (= 1.3), where F_{60} is the flux expressed in Jy at $60\,\mu$m, indicates a negligible contribution from interstellar contamination, according to Ivezić & Elitzur (1994). Therefore the presence of a detached shell is definitely required in order to explain the far-IR excess.

In the following sections we will approach the problem of reproducing the observed SED of UU Aur by assuming that a large amount of cool dust in the outer part of the shell is actually responsible for the observed flux excess at the longer wavelengths.

8. Detached shell models for UU Aurigae

As a first approach to deal with the phenomena of non-constant mass loss, we kept the common assumption that the number density of the dust grains follows a r^{-2} law, allowing the value of the inner radius of one dust component to vary. We considered an inner shell with the same features as those of the model shown in Fig. 3, that is, composed of AC and SiC. To mimic the presence of a detached shell we added a third component, and we searched for the best-fit varying the values of the inner radius from 100 to $4000\,R_*$. The outer radius of the inner shell was set equal to the inner radius of the outer shell.

8.1. A detached shell of silicate grains

Due to the emissivity law in λ^{-2} of the silicate grains, we found it difficult to reproduce both the far-IR and the sub-mm broadband photometry. Models which fit the sub-mm broadband photometric measurement do not reproduce the IRAS broadband photometry satisfactorily.

Fig. 4 shows 12 models including a silicate detached shell which fully accounts for the observed flux at 0.8 mm. These models were obtained by fixing a value for the inner and outer radius, and then looking for a model which reproduces the 0.8 mm measurement. The outer radius for these models is fixed to $10,000\,R_*$ ($\simeq$ 0.1 pc, left panel), $100,000\,R_*$ ($\simeq$ 1 pc, middle panel), $1,000,000\,R_*$ ($\simeq$ 10 pc, right panel). Inner radii of $500\,R_*$ (solid line), $1000\,R_*$ (dotted line), $2000\,R_*$ (long dashed line) and $4000\,R_*$ (dot-dashed line) were considered. Each of these models fully explains the measurement at 800 μm after the correction for the beam-size effect, but since this correction is dependent on the model, only the uncorrected measurement is plotted. The IRAS broadband photometry is also plotted non colour-corrected. Fig. 4 helps us to understand that, in order to reproduce the SED at longer wavelengths, it is required to assume a (relatively) small value for the inner radius ($R_{\mathrm{inn}} \simeq 1000\,R_*$), a large value for the outer radius ($R_{\mathrm{out}} \gtrsim 1$ pc) and a very large amount of dust (a few units in $10^{-8}\,M_\odot\,\mathrm{yr}^{-1}$).

The fits of Fig. 4 can clearly be improved by changing the values for the inner radius of the detached shell, and the value of the outer radius. The solid line on the left of Fig. 5 (top and middle panels) shows the best-fit to the observed SED of UU Aur, obtained by setting $R_{\mathrm{inn}} = 1500\,R_*$, $R_{\mathrm{out}} = 100,000\,R_*$; the dust mass loss rate is $5.2\,10^{-8}\,M_\odot\,\mathrm{yr}^{-1}$. Since the (cool) detached shell emits at longer wavelengths, all these values are independent of the grain size (except for the fact that for large grains the drift velocity becomes important, see also Sect. 9). The dust grain temperature at the inner edge of the silicate shell

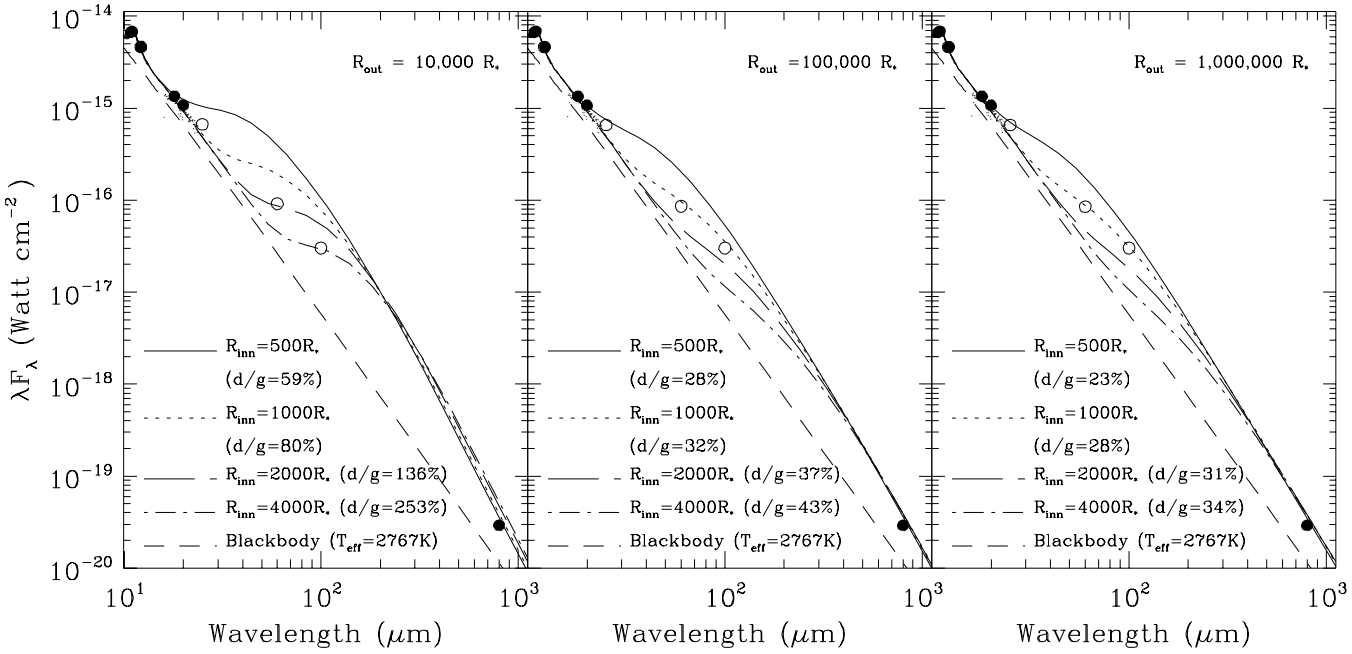

Fig. 4. Twelve models reproducing the broadband photometry at 800 μm. The inner shell is the same as in Fig. 3. The outer shell is composed of silicate, and its inner radius is set to 300 R_* (solid line), 1000 R_* (dotted line), 2000 R_* (long dashed line), 4000 R_* (dot-dashed line). All these models account for the measurement at 0.8 mm after the correction for the finite beam-size effect. IRAS broadband photometry is plotted non colour-corrected, and the measurement at 800 μm is plotted uncorrected for the finite beam-size effects. In the figure we also quote the dust-to-gas ratios of the detached shell for the different models, calculated by assuming that the rate measured via CO lines reflects the mass loss in the outer regions of the envelope

is $\sim$ 50 K. At 25, 60, 100 and 800 μm the ratio between observed and predicted flux is 0.75, 0.80, 0.95 and 1.0, respectively.

The situation would be slightly different if we assumed that a substantial fraction of the flux measured at 0.8 mm is to be ascribed to molecular emission lines. The solid line in the top and middle right panels of Fig. 5 shows the best-fit obtained by requiring to explain at least 50 % of the flux observed at 0.8 mm, and by setting the outer radius to $100,000\ R_*$. The inner radius is 500 R_* and the dust mass loss rate is $1.4\ 10^{-8}\ M_\odot\ \mathrm{yr}^{-1}$. This model accounts for 65 % of the observed sub-mm flux. At 25, 60, and 100 μm, this fit is relatively poor: at these wavelengths, the ratio between predicted and observed flux is 0.85, 1.25, 0.90, respectively.

8.2. A detached shell of amorphous carbon grains

Fig. 6 shows a fit obtained by considering an inner shell composed of AC and SiC, and an outer shell composed only of AC. The parameters of the inner shell are the same as those of the model presented in Sect. 7, while the outer shell of AC has an inner radius of 300 R_*, and dust mass loss rate of $7.2\ 10^{-9}\ M_\odot\ \mathrm{yr}^{-1}$. The dust grain temperature at the inner radius is 170 K. At 0.25, 0.60, 100, and 800 μm the ratio between predicted and observed flux is 0.95, 0.95, 1.15 and 0.95, respectively.

The value of the outer radius was set to $10,000\ R_*$. By reducing it to $3,000\ R_*$, we found that the best-model parameters (inner radius and dust mass loss rate) are the same as in the previous case, and the predicted flux at 100 and 800 μm is 90 % and 70 % of that observed. Setting the outer radius to $50,000\ R_*$, the model predicts a flux which is 130 % of that observed at 800 μm. At the other wavelengths these two models are almost identical to that shown in Fig. 6. The value of the outer radius for a C-rich detached shell is therefore quite undetermined, but is likely ranging from few thousands to few tens of thousand stellar radii.

9. Discussion

The models including a detached shell composed of silicate dust grains, with opacity law $\propto \lambda^{-2}$, do not allow one to reproduce the SED of UU Aur at longer wavelengths so well as the model with a C-rich detached shell. In fact, the models with a detached O-rich shell could be improved upon by forcing the absorption cross-sections for silicate to behave as λ^{-1}, instead of λ^{-2}. This has been previously tried by several authors (e.g., Willems & de Jong 1988, Chan & Kwok 1988, Justtanont & Tielens 1992, Griffin 1993). We ruled out this approach though, since we would get a set of optical constants which do not respect the Kramer-Kroenig relationships. Furthermore, the numerical results of the analysis (basically the dust mass loss rate for silicate) would be meaningless, since they are strongly dependent on the (arbitrary) starting wavelength from which one decides

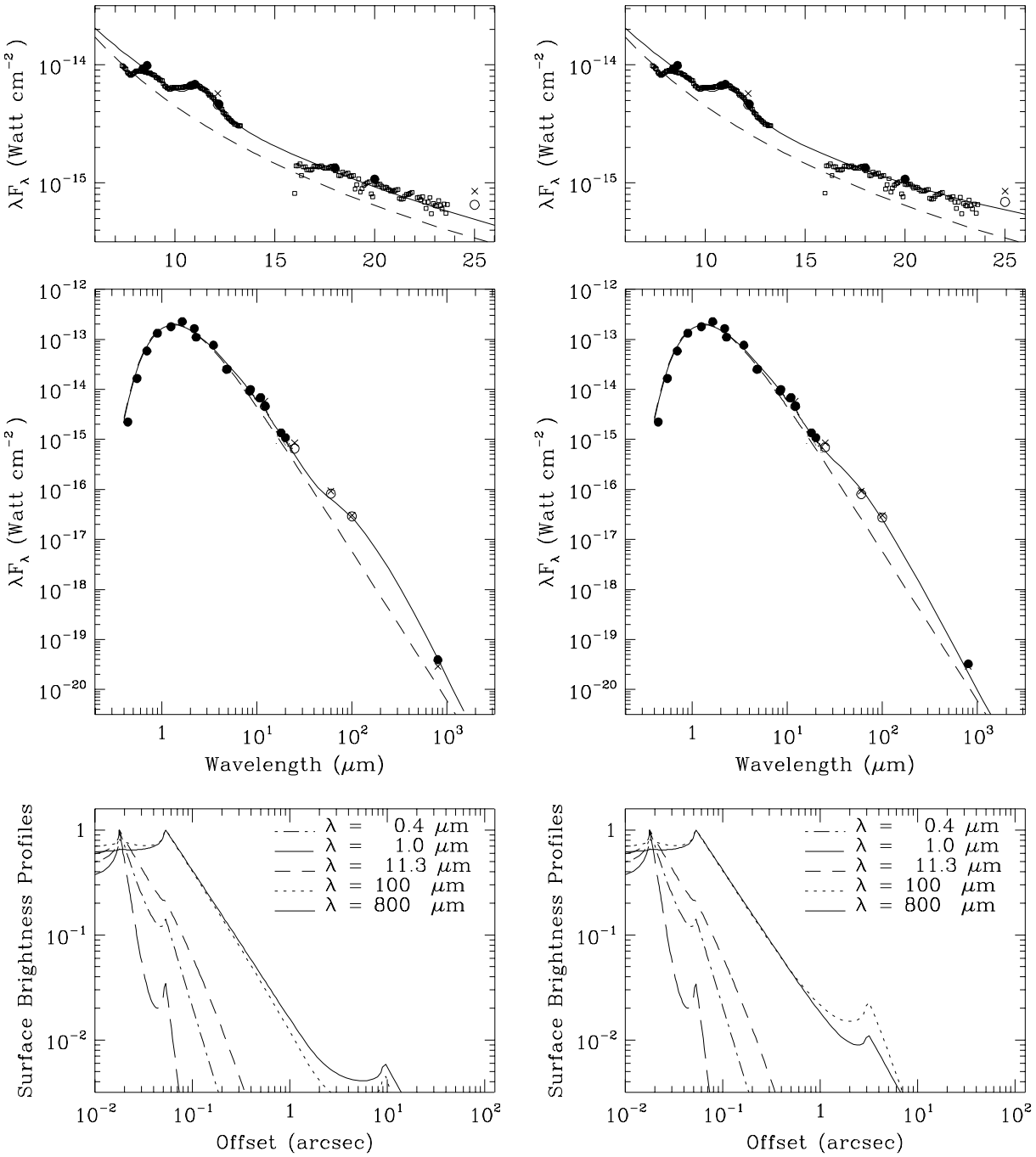

Fig. 5. Left. Top and middle panels: the solid line shows a model with a silicate detached shell, with inner radius of 1500 R_*, outer radius of 100, 000 R_*, and dust mass loss rate of 5.2 10^{-8} $M_\odot$ yr^{-1}. Bottom panel: the surface brightness profiles corresponding to the model represented above. **Right.** Top and middle panels: the solid line shows a model with a silicate detached shell which accounts for the 65 % of the flux at 0.8 mm. The inner radius of the detached shell is 500 R_*, the outer radius is 100, 000 R_*, and the dust mass loss rate is 1.4 10^{-8} $M_\odot$ yr^{-1}. Bottom panel: the normalised surface brightness profiles, at various wavelengths, for the model represented above

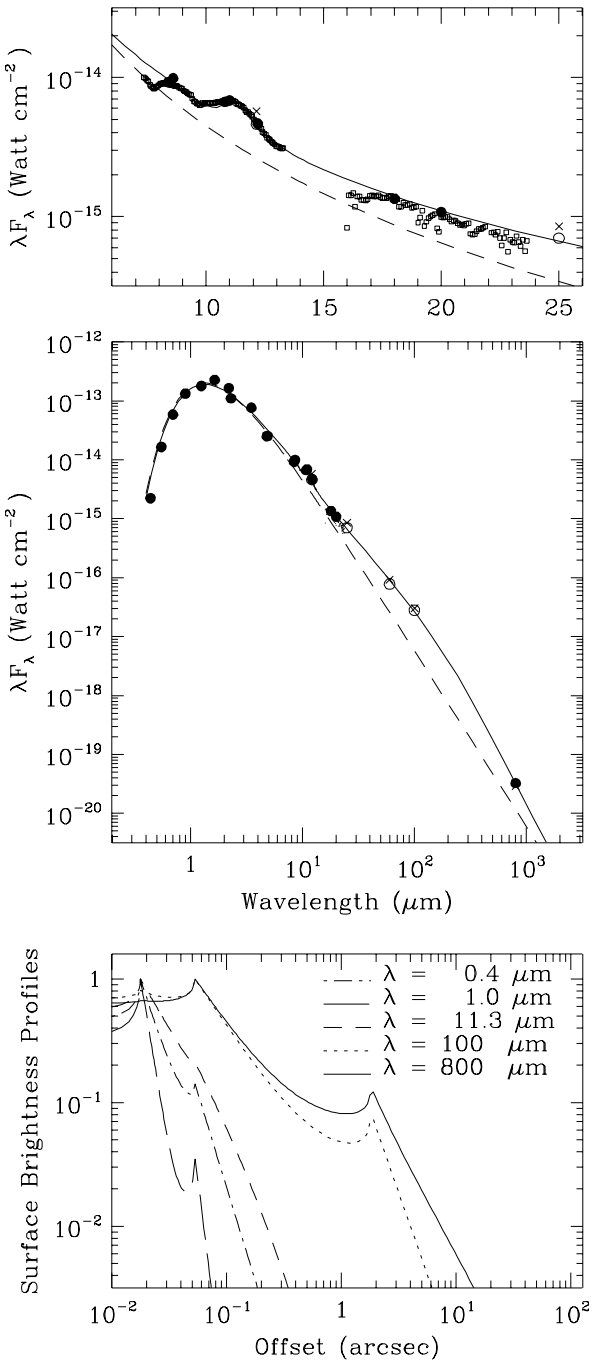

Fig. 6. A double shell model for UU Aur. The inner shell is composed of AC and SiC grains; the outer shell is composed of AC and its inner radius is 300 R_*. Top and middle panels show the fit to the observed SED. Keys to the symbols are the same as Fig. 3; the cross (filled circle) at 0.8 mm is the photometric measurement uncorrected (corrected) for the beam-size effect. Bottom: the corresponding surface brightness profiles

to force the extinction coefficients to follow a pre-defined power law in λ.

Strictly speaking, the only model which produces a fit with $\chi^2_{\rm FIR} < 1$ is the one obtained with the outer shell composed of AC. It might be argued though whether this can demonstrate that UU Aur is surrounded by a C-rich detached shell rather than an O-rich one. Indeed, the small number of observational data compared to the number of free parameters prevent us from rigorously applying the statistical test of χ^2. There are more free parameters than observational data.

The predicted surface brightness profiles (see bottom of Figs. 5 and 6) show that IR imaging techniques could not help to distinguish between the models. At longer wavelengths, using, e.g., the Plateau de Bure interferometer (France) – which achieves an angular resolution of 0.6 arcsec at 1.3 mm – one might be able to observe the inner radius of the outer shell composed of AC, but the radiation emitted at the inner radius of an outer silicate shell would be too faint to be detected.

It could be possible to discriminate between the models by comparing the dust-to-gas ratios derived for the outer shells to the cosmic abundances of the elements which compose the dust grains. However, it should be discussed first whether the gas mass loss rate measured via CO molecular line is to be related to the inner regions of the envelope or to the detached shell.

By assuming that for UU Aur the CO line measurements probe the inner regions of the shell, the dust mass loss rates of the inner shell correspond to a dust-to-gas ratio of 0.05 % for the SiC, and of 0.15 % for AC. These values – which were derived by adopting the distance and gas mass loss rate given by Olofsson et al. (1993) – could be under or over estimated by 50 %, depending on the choice of distance and gas mass loss rate (see Table 1). If the mass loss rate measured via CO line detection reflects that one of the inner regions of the shell, then the value of the dust-to-gas ratio is unusually low, compared to the cosmic abundance of Si and C. Since CO line profiles of UU Aur presented by Olofsson et al. (1993) are not double peaked, the outer shell should be so far away from the central star that CO molecules are either photo dissociated or too rarefied to be detected.

By assuming that the CO traces the outer regions of the envelope of UU Aur, the dust-to-gas ratio of the outer shell would be 40 % and 11 % for the models with an O-rich detached shell shown in Fig. 5 (left and right panels, respectively) and 5.5 % for the model with a detached shell formed of AC, shown in Fig. 6. As for the inner shell, these values could be under or over estimated by 50 %, depending on distance and gas mass loss rate. Moreover, if we adopt a grain size of 0.25 μm, the resulting dust mass loss rate in the outer shell (and the dust-to-gas ratio as well) may be further underestimated by a factor 2 because of the drift velocity of the dust grains. Table 2 summarises our estimates of all the parameters for the various cases.

If the measured gas mass loss rate corresponds to the outer shell, it clearly turns out that the value of the dust-to-gas ratio of the models including a silicate detached shell is too high, compared to the cosmic abundance of the elements which are expected to form the silicate grains in the circumstellar environ-

Table 2. A summary of the parameters of the models discussed in Sect. 8. Column 2 gives the value of the inner radius of the dust component specified in Column 1. Column 3 gives the dust mass loss rate and column 4 the dust-to-gas ratio. Columns 5–8 give the ratio between the flux predicted by the model and the observed flux. Column 9 quotes the figure numbers of the relevant models

	$R_{\rm inn}$	$\dot{M}_{\rm d}$	dust-to-gas	$F_\lambda^{\rm model}/F_\lambda^{\rm obs}$				
Dust Component	(R_*)	($10^{-10}\,M_\odot\,{\rm yr}^{-1}$)	ratio (%)	25 μm	60 μm	100 μm	800 μm	Fig.
inner shell: SiC	3	0.6 – 0.9	0.03 – 0.07 *					
inner shell: AC	9	1.9 – 2.7	0.09 – 0.20 *					
O-rich detached shell	1500	500 – 1400	24 – 125 **	0.75	0.80	0.95	1.0	5 Left
O-rich detached shell	500	130 – 380	6 – 30 **	0.85	1.25	0.95	0.65	5 Right
C-rich detached shell	300	70 – 200	3 – 17 **	0.95	1.15	0.95	0.95	6

* Derived by assuming that CO line observations probe the inner shell, that is, they measure the present-day gas mass loss rate.
** Derived by assuming that CO line observations probe the detached shell, that is, they measure a previous episode of mass loss.

ments (Mg, Fe, Si, O), therefore the model including an O-rich detached shell has to be ruled out. The inconsistency of the derived dust-to-gas ratio could be slightly reduced by adopting a smaller stellar distance. Indeed, the quantity derived via spectral analysis is $\dot{M}_{\rm d}/d_*$ (see Sect. 2.4), and the one derived via CO line detection is $\dot{M}_{\rm g}/d_*^2$. Therefore, the dust-to-gas ratio can be scaled like $1/d_*$. By adopting a distance of 250 pc (the lower limit from the parallax measurements), the stellar luminosity would be $\simeq 5250\,L_\odot$ and the dust-to-gas ratios would be reduced by 20 % only.

The dust-to-gas ratio for the model including a C-rich detached shell is also rather high. The lower limit of 3 % derived for this quantity is indeed larger than what is expected from the cosmic abundance of C, but it could be reduced further if the values of the adopted extinction coefficients were underestimated (see Sect. 3.1).

Justtanont et al. (1994) developed a theoretical model for gas kinetic temperature of circumstellar envelopes, and they applied it to three O-rich stars. They concluded that the CO mass loss rate derived from $J = 2-1$ and $J = 1-0$ transitions measures the gas mass loss rate in the outer parts of the envelopes. By assuming that also for UU Aur the rate measured via CO emission lines reflects the (high) mass loss of the outer shell, rather than the (low) mass loss in the inner shell, the lack of a clear double peaked CO line profile could be explained by the fact that the outer shell is too near to the star to allow one to see a double peaked profile. Under this assumption, the comparison of the dust-to-gas ratios derived for the O-rich and C-rich detached shells seems in favour of this latter case. Moreover, it should be noted that a value of the order of $1000\,R_*$ (that is, ~ 0.01 pc) for the inner radius of the outer shell does not match the typical value of 0.1 pc expected from the scenario of stellar evolution describing the detached shells as O-rich (Egan & Leung 1991). Instead, the value of $300\,R_*$ – derived from the best-fit with a C-rich detached shell – is consistent with the hypothesis of a short-time scale modulation in the mass loss rate.

The results of our analysis suggest us the following picture of UU Aur: we are looking at a C-rich star presently undergoing an episode of very low mass loss rate ($< 10^{-8}\,M_\odot\,{\rm yr}^{-1}$), with a C-rich detached circumstellar envelope produced by a previous episode of higher mass loss rate ($\sim 10^{-7}\,M_\odot\,{\rm yr}^{-1}$), which lasted for $10^3 - 10^4$ years, and ended a few hundred years ago. The total amount of mass ejected during this period is less that $0.01\,M_\odot$.

10. Conclusions

We carried out a detailed analysis of the observed spectral energy distribution of the carbon-rich star UU Aurigae, in order to obtain an insight on the nature of its circumstellar envelope.

A two-component model including a dust shell composed of amorphous carbon and silicon carbide, and produced by constant mass loss rate, allows us to reproduce the near-IR photometry as well as the mid-IR spectrum, but it *does not* explain the observed SED at far-IR and sub-mm. We assumed that a discontinuity in the dust grain spatial density distribution is responsible for the large far-IR excess observed in the SED, and we modelled the circumstellar environment of UU Aur as composed of two shells, each of them following a r^{-2} spatial density distribution.

Amorphous carbon and silicate were considered as (alternative) candidate components of the outer shell.

Assuming that the extinction coefficients of silicate at longer wavelengths follow a λ^{-2} law, and that of amorphous carbon follow a $\lambda^{-1.3}$ law, the model including a C-rich outer shell provides a better fit to the far-IR and sub-mm data than the one including an O-rich outer shell.

Assuming that the CO line measurements probe the inner regions of the shell, then the dust-to-gas ratio of the material ejected from the star is unusually low.

Assuming that the measured gas mass loss rate corresponds to the outer regions, we found that both models require a high dust-to-gas ratio in the detached shell. The model with silicate grains, in order to fully account for the sub-mm photometry, would require a dust-to-gas ratio larger than 20 %. This value could be reduced to 6 %, if we assume that a substantial fraction of the observed flux is to be ascribed to molecular line emission. The lower limit of the dust-to-gas ratio for the best-fit obtained with a C-rich detached shell is 3 %. The inconsistency with the value expected from the cosmic abundance of C might be ascribed to uncertain model calculations of CO emission, and to uncertain values of the extinction coefficients of AC.

For both models, the value derived for the inner radius of the outer shell is a few hundred stellar radii. Hence, the mass loss rate dropped a few hundred years ago. This is more consistent with a short time-scale modulation in the mass loss rate, than with an interruption of the mass loss for $\sim 10^4$ years corresponding to the one-time transition from the O-rich to the C-rich phase (see Sect. 1).

We propose that the outer dust shell of UU Aurigae, rather than representing a remnant of the star's former O-rich phase, instead represents a past episode of higher mass loss rate as a C-star.

Acknowledgements. Research at Armagh Observatory is grant-aided by the Dept. of Education for N. Ireland, while partial support is provided in terms of both software and hardware by the STARLINK Project which is funded by the UK PPARC. S.B. thanks STScI for a grant under the Visitor Program, which greatly facilitated this work; M.C. thanks the EU for funding via the COMETT programme. The JCMT and UKIRT are operated by the Royal Observatory Edinburgh on behalf of PPARC. The authors thank M. Barlow, I.P. Griffin and K. Mitrou for many useful comments and suggestions, and Tom Geballe and Goeran Sandell for excellent support during the observations on Mauna Kea. This research has made use of the Simbad database, operated at CDS, Strasbourg, France.

References

Avery L.W., Amano T., Bell M.B., et al., 1992, ApJS 83, 363
Bagnulo S., Doyle J.G., Griffin I.P., 1995, A&A 301, 501
Bergeat J., Sibille F., Lunel M., Lefèvre J., 1976, A&A 52, 227
Baron Y., de Muizon M., Papoular R., Pégourié B., 1987, A&A 186, 271
Blanco A., Fonti S., Rizzo F., 1991, Infrared Phys. 31, 167
Borghesi A., Bussoletti E., Colangeli L., De Blasi C., 1985, A&A 153, 1
Borghesi A., Bussoletti E., Colangeli L., et al., 1986, Infrared Phys. 26, 37
Bussoletti E., Colangeli L., Borghesi A., Orofino V., 1987, A&AS 70, 257
Chan S.J., Kwok S., 1988, ApJ 334, 362
Chan S.J., Kwok S., 1990, A&A 237, 354
Colangeli L., Mennella V., Palumbo P., Rotundi A., Bussoletti E., 1995, A&AS 113, 561
Day K.L., 1981, ApJ 246, 110
Dorschner J., Begemann B., Henning Th., Jager C., Mutschke H., 1995, A&A 300, 503
Draine B.T., 1985, ApJS 57, 587
Draine B.T., Lee H.M., 1984, ApJ 285, 89
Egan M.P., Leung C.M., 1991, ApJ 383, 314
Fernie J.D., 1983, ApJS 52, 7
Frogel J.A., Persson S.E., Cohen J., 1980, ApJ 239, 495
Griffin I.P., 1993, MNRAS 260, 831
Groenewegen M.A.T., 1995, A&A 293, 463
Groenewegen M.A.T., 1997, A&A (in press)
Groenewegen M.A.T., de Jong T., van der Bliek N.S., Slijkhuis S., Willems F.J., 1992, A&A 253, 150
Haisch B.M., 1979, A&A 72, 161
Hawkins G.W., 1990, PhD Thesis, University of California, Los Angeles
Ivezić Ž., Elitzur M., 1994, ApJ 445, 415
Joint IRAS Working Group, 1986, IRAS catalogues and atlases, Low Resolution Spectrograph (LRS), A&AS 65, 607
Joint IRAS Working Group, 1986, IRAS catalogues and atlases, IRAS Point Source Catalog, US Governement Printing Office, Washington
Joint IRAS Working Group, 1986, IRAS catalogues and atlases, Explanatory Supplement, US Governement Printing Office, Washington
Justtanont K., Tielens G.G.M., 1992, ApJ 389, 400
Justtanont K., Skinner C.J., Tielens G.G.M., 1994, ApJ 435, 852
Kastner J.H., 1992, ApJ 401, 337
Kim S.-H., Martin P.G., Hendry P.D., 1994, ApJ 422, 164
Knapp G.R., 1986, ApJ 311, 731
Koike C., Hasegawa H., Manabe A., 1980, Ap&SS 67, 495
Koike C., Kaito C., Shibai H., 1994, MNRAS 268, 321
Krüger D., Gauger A., Sedlmayr E., 1994, A&A 290, 573
Laor A., Draine B.T., 1993, ApJ 402, 441
Le Bertre T., 1988a, A&A 190, 79
Le Bertre T., 1988b, A&A 203, 85
Lorenz-Martins S., Lefèvre J., 1993, A&A 280, 567
Lorenz-Martins S., Lefèvre J., 1994, A&A 291, 831
Loup C., Forveille T., Omont A., Paul J.F., 1993, A&AS 99, 291
Mathis J.S., Rumpl W., Nordsieck K.H., 1977, ApJ 217, 425
Noguchi K., Kawara K., Kobayashi Y., Okuda H., Sato S., 1981, PASJ 33, 373
Olofsson H., Eriksson K., Gustafsson B., 1987, A&A 183, L13
Olofsson H., Carlström U., Eriksson K., Gustafsson B., Willson L.A., 1990, A&A 230, L13
Olofsson H., Carlström U., Eriksson K., Gustafsson B., 1992, A&A 253, L17
Olofsson H., Eriksson K., Gustafsson B., Carlström U., 1993, ApJS 87, 267
Papoular R., 1988, A&A 204, 138
Pégourié B., 1988, A&A 194, 335
Preibisch T., Ossenkopf V., Yorke H.W., Henning T., 1993, A&A 279, 577
Phillip H.R. and Taft, E. A., 1969, Proc. Conference on Silicon Carbide, O'Connor J. and Smiltens S. (eds.), Pergamon Press
Quirrenbach A., Mozurkewich D., Hummel C.A., Busher D.F., Armstrong J.T., 1994, A&A 285, 541
Rouleau F., Martin P.G., 1991, ApJ 377, 526
Savage B.D., Mathis J.S., 1979, ARA&A 17, 73
Seab C.G., Snow T.P., 1989, ApJ 347, 479
Skinner C.J., Whitmore B., 1988, MNRAS 235, 603
Sorrel W.H., 1990, MNRAS 243, 570
Tanabe T., Nakada Y., Kamijo F.,Sakata A., 1983, PASJ 35, 397
Thronson H.A. Jr, Latter W.B., Black J.H., Bally J., Hacking P., 1987, ApJ 322, 770
Tsuji T., 1981, J. Astrophys. Astr. 2, 95
Unno W., Kondo M., 1976, PASJ 28, 347
van der Veen W.E.C.J., Habing H.J., 1988, A&A 194, 125
van der Veen W.E.C.J., Omont A., Habing H.J., Matthews H.E., 1995, A&A 295, 445
Vassiliadis E., Wood P.R., 1993, ApJ 413, 641
Willems F.J., de Jong T., 1986, ApJ 309, L39
Willems F.J., de Jong T., 1988, A&A 196, 173
Yamashita Y., 1972, Tokyo Astron. Obs. Ann. 13, 169
Zuckerman B. 1993, A&A 276, 367

This article was processed by the author using Springer-Verlag LaTeX A&A style file *L-AA* version 3.